Geology of the Precambrian rocks between Elizabethtown and Mineville, eastern Adirondacks, New York

TIBOR GASPARIK *Department of Earth and Space Sciences, State University of New York, Stony Brook, New York 11794*

ABSTRACT

The northern part of the Elizabethtown and Port Henry quadrangles, which includes the largest surficial exposure of olivine metagabbro in the Adirondack Precambrian rocks, was mapped at a scale of 1:15,840. The area is dominated by meta-igneous rocks of four types, which probably intruded in the following sequence (from earliest to latest): granitic gneiss, anorthosite, garnet-pyroxene gneiss, and metagabbro. The metagabbroic complex is a multiple intrusion forming a basinlike structure, with the central part still covered by a roof complex of granitic gneisses. The limited scale of the in situ differentiation could not produce the observed range of compositions; therefore, differentiation prior to intrusion is postulated. The observed differentiation trend toward lower silica content can be explained by pyroxene fractionation. Intrusive relationships are evident from locally preserved chilled margins in gabbros and from the development of hybrid zones in the surrounding granitic gneisses; these zones are especially common in the roof complex. Granulite facies metamorphism produced garnet-bearing mineral assemblages, but igneous assemblages and textures are still well preserved.

The garnet-pyroxene gneiss is characterized by the metamorphic assemblage plagioclase + garnet + clinopyroxene and by the presence of blue plagioclase megacrysts. The gneiss forms intrusive sill-like bodies, usually in contact with anorthosite. In some places, the contact is transitional, suggesting a possible comagmatic origin.

INTRODUCTION

Geologic mapping in the eastern Adirondacks was done as part of a detailed study of the Elizabethtown metagabbroic complex. The area in the northern part of the Elizabethtown and Port Henry quadrangles was originally mapped by Kemp and Ruedemann (1910) and was remapped by Walton (1948–1960). Geologic mapping of about 160 km² was done in the summers of 1977 and 1978 on enlargements of 15-minute topographic maps at a scale of 1/15,840. The geologic features were later redrawn onto new 7½-minute topographic maps.

This paper presents results of the field work and gives characteristics of the major rock types in the area. The new geologic map is shown in Figure 1. Figure 2 includes the Quaternary cover and shows only the geologic features actually observed in the field. Measurements of the foliation attitudes are presented in Figure 3.

GEOLOGY AND ROCK TYPES

The area is part of a large synformal structure with continuations into the Ausable Forks quadrangle on the north and the Paradox Lake quadrangle on the south. Precambrian metamorphic rocks are almost entirely of four major types: (1) metagabbro, (2) garnet-pyroxene gneiss, (3) anorthosite, and (4) granitic gneiss.

The relative sequence of intrusions is difficult to estimate because most of the intrusive relations have been obliterated by deformation. The granitic gneiss can be considered the oldest rock type because hybrid zones are commonly developed along contacts with both the anorthosite (for example, west and southwest of North Pond) and the metagabbro (for example, Campbell Mountain).

The younger age of the metagabbro relative to the granitic gneiss is also indicated by the development of chilled zones in contacts with the granitic gneiss. A chilled margin has been observed on the northern slope of Hoisington Mountain. Very fine-grained metagabbro in sharp contact with the granitic gneiss passes gradually into a typical metagabbro within a distance of 10 m. Contact effects on the granitic gneiss are negligible.

The field relations between the anorthosite and the garnet-pyroxene gneiss are well defined. The gneiss contains anorthosite xenoliths, clearly indicating that the host rock intruded after solidification of the anorthosite. Metagabbroic bodies are usually surrounded by the granitic gneiss; thus, direct contacts between the metagabbro and the anorthosite or the metagabbro and the garnet-pyroxene gneiss are rare. The metagabbro is most probably younger than both the anorthosite and the garnet-pyroxene gneiss, but convincing field evidence has not been found in the area of study.

The assumed age sequence of intrusions is not reflected in the usual vertical sequence of major rock types. The typical sequence from depth to the surface is anorthosite–(garnet-pyroxene gneiss)–granitic gneiss–metagabbro–granitic gneiss.

Metasedimentary rocks have been found in only a few outcrops and thus were not mapped as separate units. Biotite schist, quartzite, and calc-silicate have been found as inclusions in the anorthosite, usually near contacts with the granitic gneiss, and in the garnet-pyroxene gneiss. It is suspected that metasedimentary rocks also occur in the granitic gneiss, but they have not been recognized in the field.

The density of metagabbros is significantly higher (3.0 to 3.4 g/cm³) than the density of anorthosites (≈ 2.8 g/cm³) or granitic gneisses (≈ 2.7 g/cm³), so the distribution of metagabbroic bodies can be determined by a gravity survey. The gravity contours in Figure 4 were taken from the Bouguer gravity anomaly map of northern New York (Simmons and Diment, 1973). The gravity contour pattern clearly correlates with the surficial extent of metagabbros. If the pattern reflects the distribution of metagabbros in the area, then the main volume of metagabbros would be situated between New Russia and Mineville. The granitic gneiss cropping out in this part of the area probably represents the roof that covers the main part of the complex.

Faults belong mostly to the north-

Geological Society of America Bulletin, Part I, v. 91, p. 78–88, 7 figs., 1 table, February 1980, Doc. no. 00205.

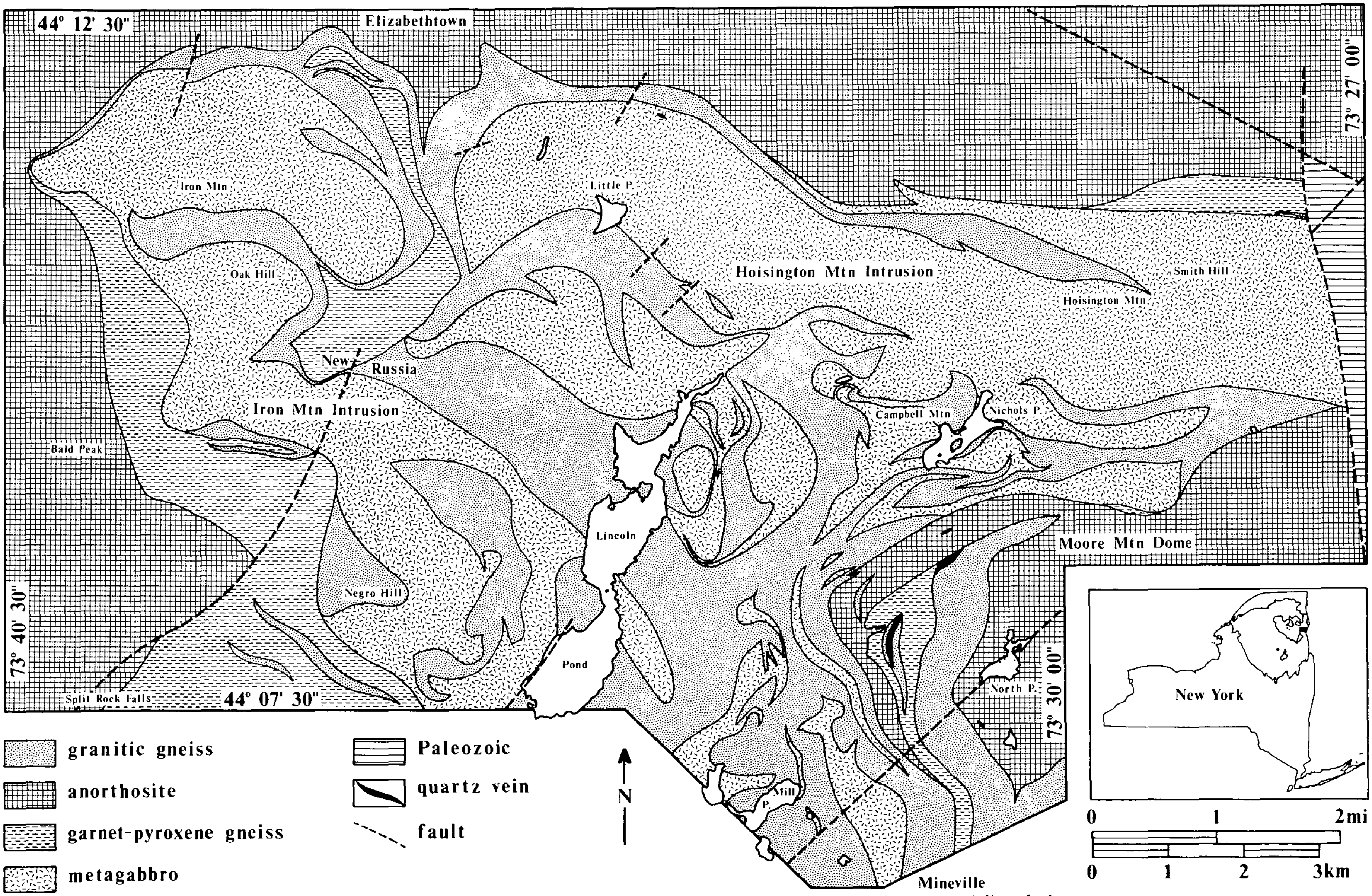

Figure 1. Bedrock geology of area between Elizabethtown and Mineville, eastern Adirondacks.

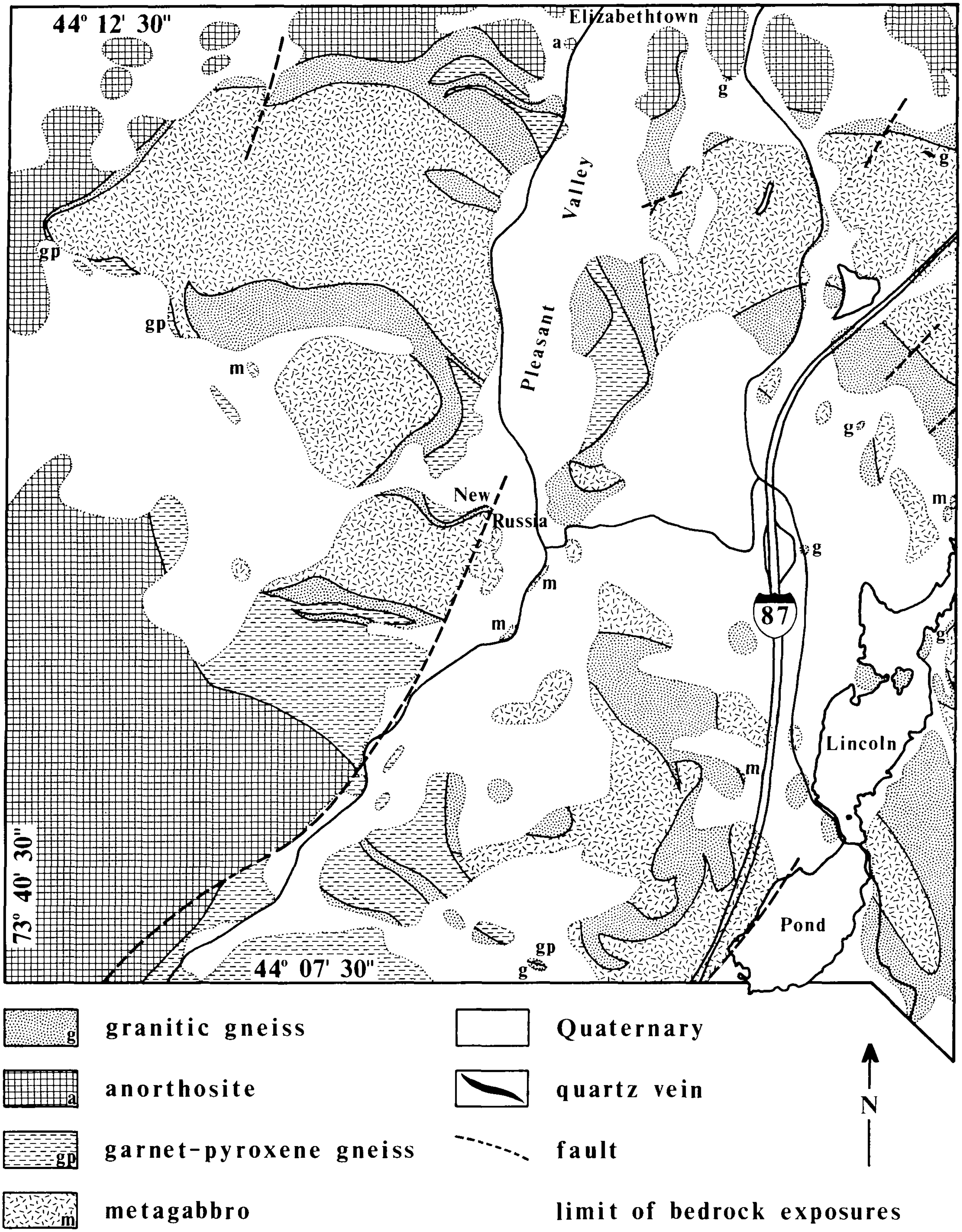

Figure 2. Geologic map of bedrock exposures.

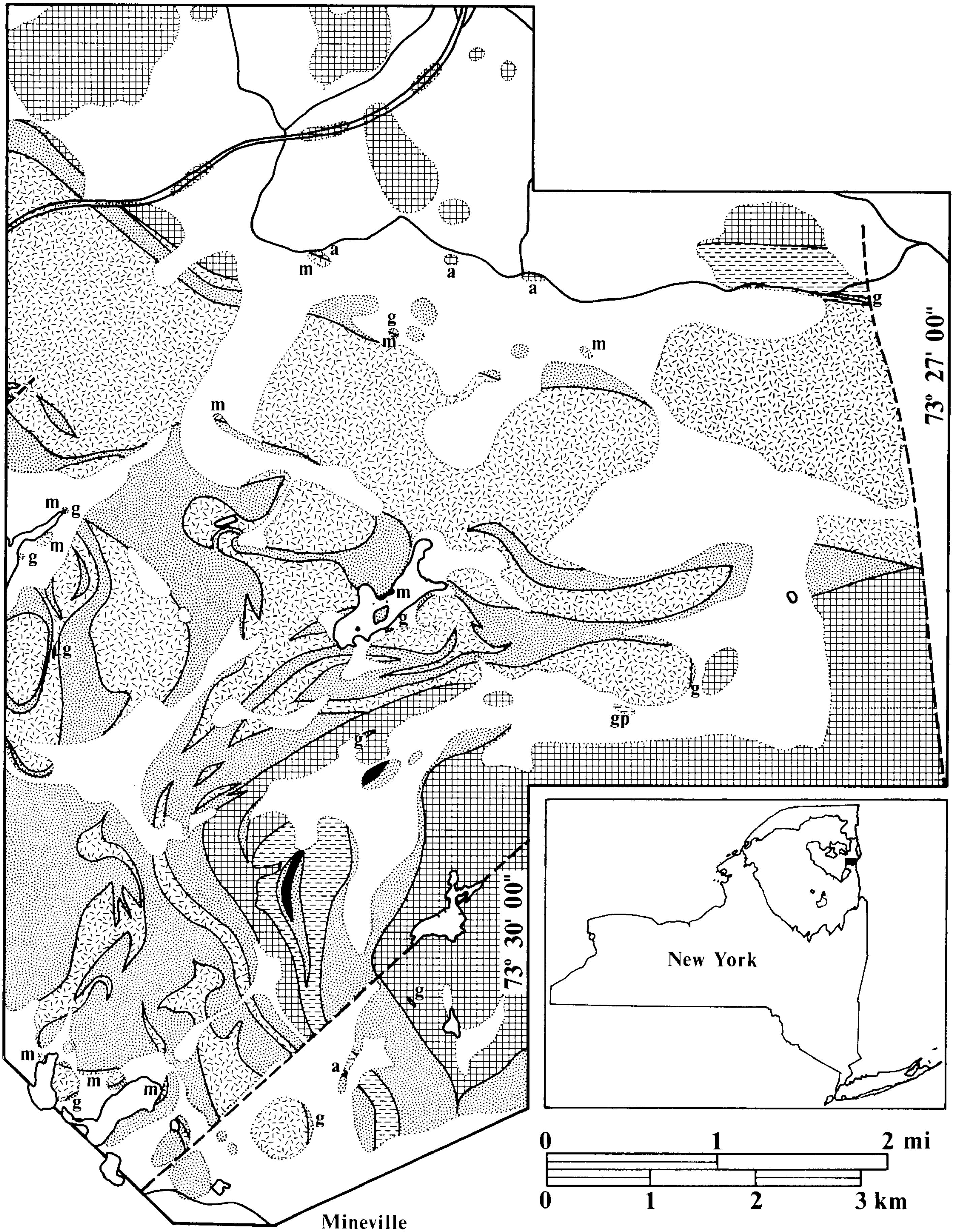

Figure 2. *(Continued).*

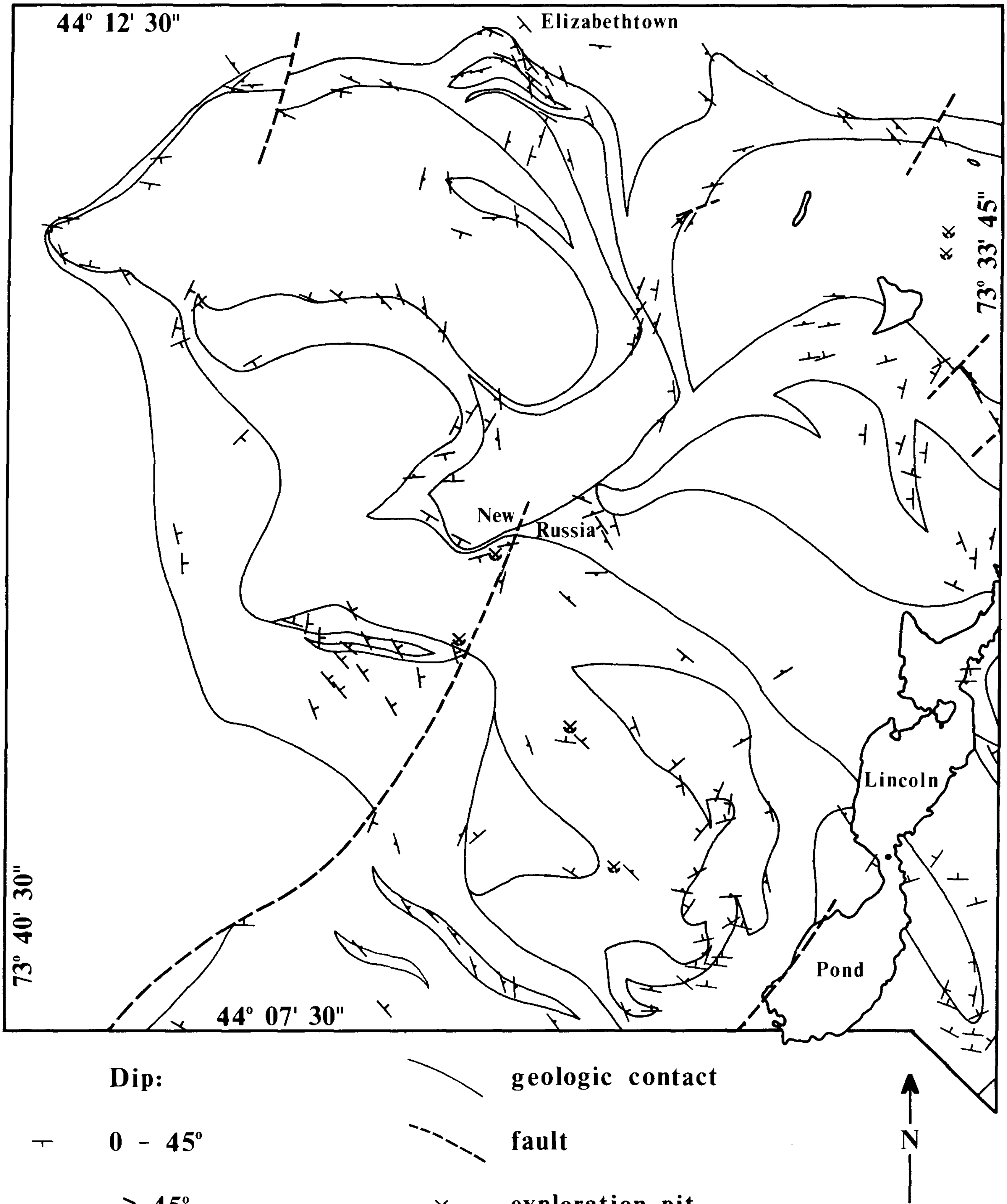

Figure 3. Foliation attitudes.

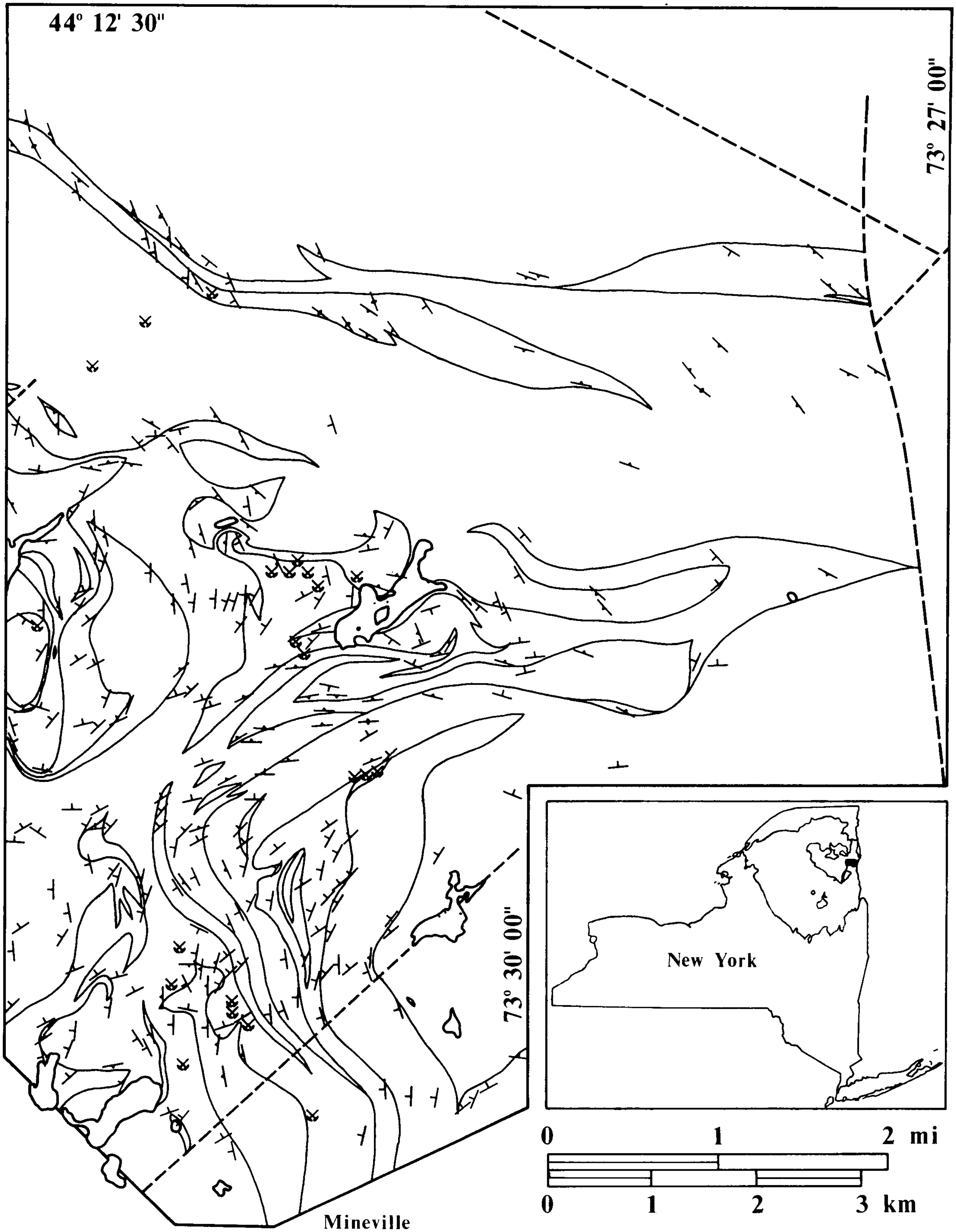

Figure 3. *(Continued).*

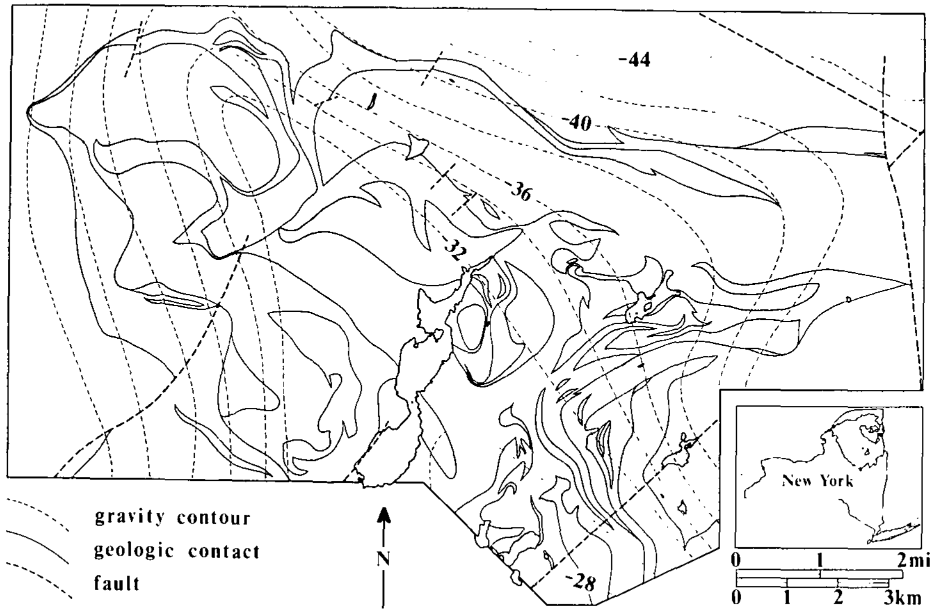

Figure 4. Bouguer gravity anomaly map. Gravity contours after Simmons and Diment (1973). Contour interval, 2 mgal.

TABLE 1. MAJOR-ELEMENT ANALYSES, NORMS, AND MODES OF ROCKS FROM THE ELIZABETHTOWN QUADRANGLE

	Metagabbros, type A								Metagabbros, type B				Ga.-px. gneiss	Anortho-site	Hybrid rocks				Granitic gneisses	
Locality*:	1	2	3	4	5	6	7	8	9	10	11	12	13	14	15	16	17	18	19	20
SiO_2	45.95	45.22	48.88	44.86	47.60	47.97	46.14	39.74	44.49	43.03	42.48	53.63	43.58	53.63	53.45	50.34	58.75	67.71	70.52	70.46
Al_2O_3	16.79	17.71	19.85	16.60	15.41	19.75	18.11	10.59	16.61	13.58	14.72	21.04	15.02	24.52	16.25	15.92	14.86	13.41	13.12	13.90
Fe_2O_3	1.69	2.67	1.49	1.97	1.62	0.80	1.61	2.65	2.46	2.62	2.90	1.22	3.86	0.57	1.97	1.81	2.78	2.83	3.26	0.90
FeO	13.15	13.40	8.37	14.96	13.43	9.07	10.16	21.48	14.52	16.27	15.26	4.57	13.59	1.60	10.68	11.15	6.72	2.76	0.60	3.61
MgO	8.18	5.01	5.34	5.89	6.17	5.98	9.36	5.83	5.81	8.31	5.69	1.85	3.40	1.66	1.91	2.62	2.01	0.79	0.49	0.32
CaO	8.15	7.98	8.92	8.78	8.30	9.21	8.17	9.04	8.68	9.30	10.20	7.83	11.69	10.90	6.97	7.53	3.83	1.68	1.06	2.19
Na_2O	2.94	3.45	3.97	2.95	3.19	3.42	3.19	2.20	2.94	2.01	2.78	4.85	2.83	4.48	3.90	4.55	3.61	3.05	3.57	3.07
K_2O	0.77	0.92	0.89	0.57	0.95	0.82	0.60	1.21	0.90	0.50	0.67	2.25	0.62	0.55	2.50	1.85	3.53	5.59	5.78	5.86
P_2O_5	0.39	0.39	0.35	0.08	0.45	0.35	0.15	2.50	0.22	0.11	0.26	0.29	1.75	0.03	0.71	1.23	0.54	0.17	0.05	0.13
TiO_2	2.20	3.86	1.84	3.92	2.90	1.58	1.09	5.38	4.26	4.94	5.67	1.44	4.21	0.31	1.85	2.42	1.57	0.68	0.37	0.48
MnO	0.20	0.18	0.13	0.21	0.21	0.15	0.15	0.35	0.23	0.24	0.24	0.08	0.26	0.04	0.17	0.20	0.14	0.07	0.02	0.06
H_2O^+	0.39	0.33	0.48	0.33	0.48	0.34	0.64	0.29	0.35	0.50	0.41	0.51	0.26	0.96	0.37	0.35	0.39	0.68	0.32	0.31
CO_2	0.55	0.25	0.44	0.25	0.21	0.20	0.06	0.26	0.19	0.11	0.19	0.23	0.27	0.52	0.45	0.14	0.14	0.10	0.55	0.18
Total	101.35	101.37	100.95	101.37	100.92	99.64	99.43	101.52	101.66	101.52	101.47	99.79	101.34	99.77	101.18	100.11	98.87	99.52	99.71	101.47
ρ (g/cm^3)	3.23	3.18	3.01	3.32	3.20	3.09	3.19	3.39	3.28	3.38	3.33	2.87	3.29	2.77	2.99	3.01	2.86	2.73	2.68	2.72

Q	..	..	..	..	..	..	..	..	..	..	..	..	..	0.75	0.81	..	12.80	26.47	27.81	25.60
Or	4.13	5.12	4.89	3.12	5.19	4.54	3.28	6.69	4.95	2.70	3.69	12.83	3.48	3.11	13.95	10.47	20.26	31.91	32.48	32.33
Ab	23.56	26.81	30.08	23.29	26.48	27.50	22.88	18.48	22.09	16.50	16.97	40.13	24.16	38.53	33.07	39.01	31.48	26.46	30.49	25.74
An	27.53	28.37	31.35	28.17	23.05	33.87	30.87	14.45	27.45	24.28	23.98	27.99	25.15	43.28	18.37	16.81	13.52	6.18	2.57	6.39
Ne	0.19	1.18	1.53	0.64	..	0.64	1.82	..	1.25	..	3.15	0.95	..	..	..	0.06	..	..	..	..
Di	6.84	6.52	7.67	11.75	12.31	6.84	5.77	12.24	11.33	17.24	21.63	7.68	19.14	8.34	9.91	11.28	1.51	0.81	2.12	2.97
Hy	..	..	..	..	6.08	..	..	1.94	..	4.63	..	..	3.45	3.37	16.45	..	13.88	4.00	0.55	4.67
Ol	30.62	21.95	18.31	24.22	19.42	22.08	31.85	29.55	23.03	24.17	17.94	5.68	10.11	..	..	13.90	..	..	..	..
He	..	..	..	..	..	..	..	..	..	..	..	..	..	..	..	..	..	..	1.09	..
Mt	1.34	2.19	1.21	1.59	1.31	0.65	1.30	2.16	2.00	2.09	2.36	1.03	3.20	0.48	1.62	1.51	2.35	2.38	0.53	0.73
Il	3.48	6.33	2.98	6.33	4.67	2.58	1.76	8.76	6.91	7.86	9.21	2.42	6.97	0.52	3.04	4.04	2.66	1.14	0.61	0.78
Ap	0.75	0.78	0.69	0.16	0.88	0.70	0.30	4.97	0.44	0.21	0.52	0.59	3.53	0.06	1.42	2.50	1.11	0.35	0.10	0.26
Cc	1.58	0.74	1.29	0.73	0.61	0.59	0.18	0.77	0.56	0.32	0.56	0.70	0.81	1.58	1.34	0.42	0.43	0.31	1.65	0.53
An (%)†	53.89	51.41	51.03	54.74	46.53	55.19	57.43	43.89	55.41	59.54	58.56	41.09	51.01	52.90	35.71	30.12	30.04	18.92	7.78	19.89
Mg#	0.47	0.34	0.47	0.36	0.40	0.50	0.56	0.28	0.36	0.42	0.34	0.34	0.24	0.56	0.20	0.25	0.26	0.19	0.18	0.10
Quartz	..	..	..	..	..	..	..	..	..	..	..	..	0.3	0.4	8.4	..	15.2	23.2	19.7	23.8
Microperthite	tr.	tr.	..	..	..	..	..	tr.	tr.	..	..	0.1	..	..	15.5	6.5	20.9	42.7	60.0	46.6
Plagioclase	33.2	56.7	59.3	44.2	33.0	59.9	36.6	25.8	41.0	56.5	16.8	75.6	42.3	90.6	41.4	52.6	34.4	23.4	13.4	20.5
Olivine	8.8	2.9	11.1	1.2	3.0	..	..	10.6	..	..	..	..	..	..	..	..	..	..	..	..
Cpx (primary)	10.2	2.8	3.3	8.7	8.7	1.3	1.9	15.0	1.7	14.5	30.9	12.6	..	..	..	..	..	..	..	..
Cpx (metamorphic)	7.6	6.7	9.1	8.3	13.0	8.3	5.0	14.3	12.1	3.4	10.6	1.5	27.8	4.6	..	18.9	..	..	..	..
Orthopyroxene	2.5	1.8	1.4	0.9	0.7	2.7	3.4	tr.	2.5	0.9	0.6	..	tr.	..	..	..	..	..	..	..
Garnet	20.3	14.3	11.5	18.1	16.8	17.0	17.5	0.4	21.5	8.0	7.6	4.0	16.7	..	4.6	..	0.9	0.1	..	4.7
Amphibole	8.4	6.9	1.0	5.2	14.3	4.8	24.8	20.1	6.5	6.0	27.6	3.3	0.1	..	18.0	18.0	15.8	8.1	..	2.6
Biotite	3.6	1.6	0.9	5.3	6.4	4.0	0.2	..	5.9	4.8	0.1	0.1	0.2	0.5	0.1	0.1	..	..	..	0.1
Opaques	3.7	5.6	0.5	7.8	3.0	0.5	0.4	8.5	8.6	4.5	5.7	2.0	8.8	0.1	2.6	3.8	2.4	0.9	3.0	0.4
Spinel**	0.2	0.6	1.0	tr.	0.2	0.9	0.7	..	tr.	0.8	..	tr.	..	..	..	..	..	..	..	..
Apatite	1.4	0.1	0.9	0.3	1.1	0.7	0.1	5.3	0.2	0.6	0.1	0.8	3.7	..	0.5	0.1	1.1	0.4	..	0.1
Zircon	..	..	..	..	..	..	..	..	..	..	..	..	..	..	..	..	0.4	tr.	tr.	0.1
Sphene	..	..	..	..	..	..	..	..	..	..	..	..	..	..	..	..	..	0.1	tr.	..
Hematite	..	..	..	..	..	..	..	..	..	..	..	..	..	..	..	..	tr.	0.3	0.2	..
Carbonate	..	..	..	..	..	..	..	..	..	..	..	..	..	..	..	..	0.5	..	1.4	..
Chlorite	..	..	..	..	..	..	..	..	..	..	..	..	..	1.5	8.9	..	8.3	0.9	2.4	1.2
Serpentine	..	..	..	..	..	..	9.6	..	..	..	..	..	..	..	..	..	..	..	..	..
Clinozoisite	..	..	..	..	..	..	..	..	..	..	..	..	..	2.4	..	..	..	..	..	..
Points counted	5,220	2,403	3,128	2,662	2,834	2,912	2,847	3,035	2,356	2,884	3,010	2,465	2,805	2,323	2,616	1,770	2,207	1,886	2,155	2,182
Area (mm^2)	522	481	626	532	567	582	569	607	471	577	602	493	561	465	523	354	441	377	431	436

* See Appendix 2.

† 100 An/(An + Ab).

\# Mg/(Mg + Fe_{total}), molecular ratio.

** Plagioclase with spinel clouding was point-counted separately, and the amount of spinel was calculated by taking for an average density of spinel clouding the value of 3% (by volume) of spinel in plagioclase.

northeast–trending system, and all are normal. In a few cases in the field it was possible to demonstrate displacements along these faults. The displacements are relatively small and have only a minor effect on the outcrop pattern.

Samples of each of the major rock types have been studied petrographically and analyzed for major elements (see Appendix 1 for analytical procedures and Appendix 2 for sample localities). The following descriptions of major rock types and conclusions are based on field observations, on the results of twenty major-element rock analyses and modal analyses (Table 1), and on phase chemistry determined by the electron microprobe.

Metagabbro

The Elizabethtown metagabbroic complex is composed of two large gabbroic intrusions and a few smaller bodies situated east of Lincoln Pond. The Hoisington Mountain intrusion, 12 km long and 2 to 3 km wide, extends east from Pleasant Valley to Westport. The Iron Mountain intrusion is located mainly west of Pleasant Valley and extends southeast beyond Lincoln Pond, crossing Pleasant Valley at New Russia.

The metagabbro has well-preserved subophitic texture, with grain size ranging from very fine to coarse. The crystallization sequence of primary minerals is plagioclase → olivine → ilmenite → clinopyroxene. Metamorphic mineral assemblages formed by reaction between plagioclase, olivine, and ilmenite, producing amphibole (pargasite), biotite, garnet, clinopyroxene, orthopyroxene, and spinel. Apatite, perthite, pyrite, and chalcopyrite are present in accessory quantities.

Both primary and metamorphic plagioclase crystals are present. Primary plagioclase has preserved its original euhedral shape, but composition has changed during metamorphism from An_{40-60}, based on normative plagioclase, to An_{30-40}, determined by the electron microprobe. Grains are usually clouded with spinel inclusions. The density of spinel clouding does not exceed 10% (by volume) of plagioclase in the most densely clouded parts. The variable density of spinel clouding is believed to be related to the original zonation of plagioclase, although compositional zoning has been completely eliminated during metamorphism. Higher density of spinel clouding probably reflects the original higher anorthite content of primary plagioclase. Metamorphic plagioclase can be distinguished by relatively smaller grain size and lack of spinel clouding.

There are also two generations of clinopyroxene with the same composition. The composition of primary clinopyroxene was readjusted during metamorphism by exsolving amphibole in the form of tiny inclusions. The Fe_{total}/Mg ratio of mafic minerals determined by the electron microprobe increases in the order clinopyroxene < orthopyroxene ≈ biotite < amphibole < olivine < garnet < spinel < ilmenite in the sample from locality 1, and clinopyroxene < orthopyroxene < amphibole < biotite < olivine < garnet < ilmenite in the most differentiated sample from locality 8.

Reaction coronas around olivine and ilmenite have been observed in the coarser varieties of metagabbros. The coronas are similar to those described by Whitney and McLelland (1973) from other areas in the Adirondacks. Olivine is typically surrounded by a shell of equigranular clinopyroxene and orthopyroxene, followed by a shell of metamorphic plagioclase (sometimes missing) and an outer shell of a garnet-pyroxene symplectite. Ilmenite is usually surrounded by biotite and amphibole followed by an outer shell of a garnet-pyroxene symplectite.

Major-element rock analyses of metagabbros (Table 1, analyses 1 through 12) show mostly alkali basaltic compositions and a differentiation trend toward iron enrichment and lower silica content (Fig. 5). Differentiation in the range from centimetres to a few metres has been observed leading to two different mineral assemblages: plagioclase + olivine, with small amounts of ilmenite and clinopyroxene (type A), and plagioclase + ilmenite + clinopyroxene (type B). The in situ differentiation did not produce rhythmic layering comparable to the layering found in the Jay Mountain intrusion (Whitney, 1972) and could not result in the observed differentiation trend. Therefore, fractionation of the gabbroic magma prior to the intrusion is assumed. The differentiation trend toward lower silica content can be explained by pyroxene fractionation. Metagabbroic bodies are often cut by dikes formed by the same metagabbro as the country rock, which suggests that the intrusion of the Elizabethtown complex was not a single event but occurred in stages.

Most deformational effects are restricted to the outer margins of gabbroic intrusions. Exceptions can be found on Smith Hill in the eastern part of the Hoisington Mountain intrusion, where several northwest-trending shear zones cut across the gabbroic body. The deformation results in the development of foliation, strong amphibolitization, destruction of igneous textures, and disappearance of spinel clouding in plagioclase.

Garnet-Pyroxene Gneiss

Garnet-pyroxene gneiss was originally described by Kemp and Ruedemann (1910) as the "intermediate gabbro." Kemp and Ruedemann distinguished two types of "intermediate gabbro": the Woolen Mill type and the Split Rock Falls type. The less mafic Split Rock Falls type is more common and is considered to be the typical representative.

The garnet-pyroxene gneiss has been found in seven separate sill-like bodies. The characteristic mineral assemblage is plagioclase + pink garnet + green clinopyroxene. Variable amounts of amphibole, quartz, and K-feldspar are also typical. Apatite, ilmenite, magnetite, biotite, and or-

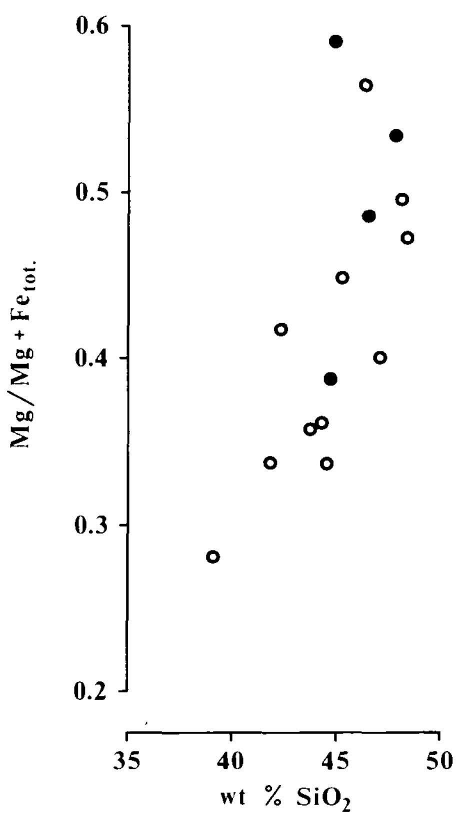

Figure 5. Variation diagram of Mg/(Mg + $Fe_{(total)}$) ratio versus SiO_2 in percent by weight for metagabbros of Elizabethtown complex. Open circles = this study; solid circles = whole-rock analyses 1, 3, 4, and 5 from Kemp and Ruedemann (1910, p. 55).

thopyroxene may be present in accessory quantities. Fine-grain and granoblastic textures are characteristic. Foliation is usually well developed, although unfoliated types are also present. The most significant feature is blue plagioclase megacrysts, 1 to 3 cm across. These megacrysts have lenticular shapes, and in most of them only the center of the crystal is blue. The megacrysts are very conspicuous on weathered surfaces because they are more resistent to weathering. Increasing deformation and recrystallization results in coarsening of the matrix and disappearance of the blue color of the megacrysts.

The garnet-pyroxene gneiss contains anorthosite xenoliths in the form of angular blocks of different sizes, showing that the intrusion is younger than the anorthosite. The best examples, described previously by Kemp and Ruedemann (1910), can be seen in the bed of the Bouquet River at Split Rock Falls.

Contacts of the gneiss with the anorthosite are mostly sharp, but in some places (for example, southwest of New Russia), gradual transitions from the garnet-pyroxene gneiss into the anorthosite have been observed. In this case, the number of plagioclase megacrysts in the gneiss gradually increases until the rock grades into anorthosite completely composed of megacrysts. The close field association of the garnet-pyroxene gneiss with the anorthosite suggests that the gneiss may represent the composition evolved from the same parent magma from which the anorthosite fractionated.

The original igneous rock from which the garnet-pyroxene gneiss formed was gabbro or norite. Metamorphic reaction between plagioclase and orthopyroxene producing clinopyroxene and garnet has, in most instances, led to a complete elimination of orthopyroxene. Therefore, the nomenclature of de Waard (1969), based on the presence of orthopyroxene, could not be applied to this rock type. Similar rocks are usually described as norite and jotunite. The field relations between norite and anorthosite in the Snowy Mountain dome (de Waard and Romey, 1969) are very similar to those observed between the garnet-pyroxene gneiss and anorthosite.

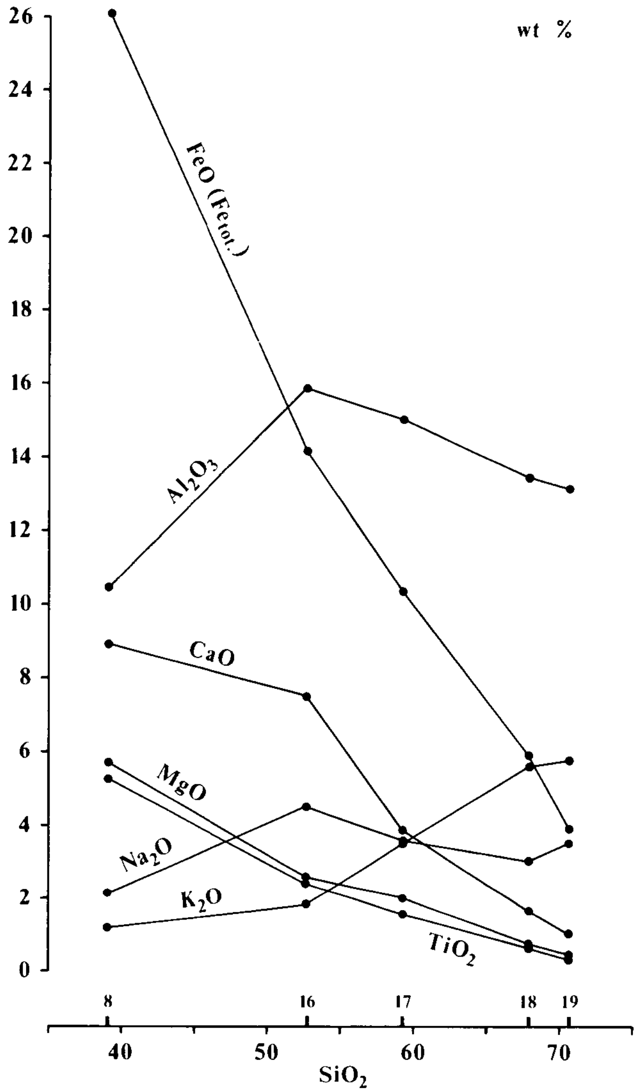

Figure 6. Variation diagram of major-element oxides versus SiO_2 (percent by weight), based on whole-rock analyses of samples from localities 8, 16, 17, 18, and 19. Sample from locality 8 is assumed gabbroic end member. Sample from locality 16 from margin of a gabbroic body near contact has bulk composition changed due to assimilation of granitic country rocks. Samples from localities 17 and 18 are hybrid rocks of granitic composition, and sample from locality 19 is a granitic gneiss with bulk composition unaffected by hybridization process. Intermediate concentrations of most major elements in hybrid rocks relative to their assumed end members support mixing model of their formation.

Anorthosite

The anorthosite of the Marcy massif surrounds the area from the north and west. A small anorthosite body in the southeastern part of the map area, completely isolated from the Marcy massif, forms the Moore Mountain dome.

Anorthosite surrounding the area from the west is composed mainly of blue plagioclase megacrysts in a granulated white plagioclase matrix. Anorthosite surrounding the area from the north and anorthosite of the Moore Mountain dome typically consist of granulated plagioclase and porphyroblasts of garnet.

Granitic Gneiss

The granitic gneiss, usually pink on the weathered surface, is mainly composed of microperthite, plagioclase, and quartz. The most common mafic mineral is hornblende. Clinopyroxene may be present, but it is less common. Other accessories are garnet, sphene, zircon, apatite, biotite, magnetite, and allanite. Orthopyroxene has not been found. Mafic content is usually very low; content of mafic minerals higher than 5% is considered to be the result of hybridization by gabbroic magma. Major-element rock analyses (Table 1, analyses 18, 19, 20) show compositions corresponding to adamellite.

The intrusion of anorthosites and gabbros at great depth led to a partial melting of the granitic gneiss and set conditions favorable for the formation of hybrid rocks. Mechanical mixing of the undersaturated gabbroic magma and the granitic gneiss could have resulted in hybrid rocks having the syenite bulk compositions that are common in the Adirondacks. Under favorable conditions, a complete suite of rocks ranging in composition from granitic to gabbroic could have developed. The mafic content of granitic gneisses, which is typically low, increases in the vicinity of contacts with metagabbros. With increasing hybridization, quartz content decreases, and plagioclase with amphibole become more abundant.

The effect of the hybridization process on the major-element bulk compositions of granitic gneisses has been studied on a suite of five samples representing two end-member compositions and three hybrid rocks (Fig. 6). In most cases, major-element contents of hybrid rocks are intermediate to those of the assumed end members, which is consistent with the mixing model of their formation.

ACKNOWLEDGMENTS

This work was carried out under the guidance of Paul H. Reitan. I am also greatly indebted to Y. W. Isachsen and P. R. Whitney for valuable discussions of field problems, A. E. Bence for use of the electron microprobe, and G. N. Hanson for critical review of the manuscript. The Society of Sigma Xi and the Graduate Student Association at the State University of New York, Buffalo, provided financial support.

APPENDIX 1. ANALYTICAL PROCEDURES

Major-element analyses were made by rapid procedures used at the Department of Geological Sciences, State University of New York at Buffalo. Replicate analyses were done for each sample, and the reported results are averages of both analyses. Standards used as references in all analyses were BR, BCR-1, T-1, GA, and GH (Flanagan, 1973). Additional standards were used for analyses of elements with concentrations falling outside the concentration ranges of the reference standards.

Most of the elements were analyzed from solutions prepared by dissolving 0.1 g of the sample material. Concentrations of SiO_2, Al_2O_3, total Fe, TiO_2, and P_2O_5 were determined using a Beckmann Model B spectrophotometer. Concentrations of CaO, MgO, MnO, Na_2O, and K_2O were determined by flame photometry, using a Perkin-Elmer Model 290 atomic absorption spectrophotometer. FeO was determined by titration. CO_2 was determined using CO_2 test tubes and H_2O^+ by the Penfield method. Densities were measured using a Beckmann Model 930 air comparison pycnometer.

The precision of analyses is satisfactory according to precision standards used at State University of New York at Buffalo. Higher sums most probably reflect a systematic weighting error.

APPENDIX 2. SAMPLE LOCALITIES

Localities are shown in Appendix Figure 1.

1. Sample 114: Metagabbro, type A, a typical representative of the rock type. Roadcut on the northwest side of Interstate 87, the first outcrop southbound from the exit to Route 9N in the metagabbro of the Hoisington Mountain intrusion, about 4 km southeast of Elizabethtown.
2. Sample 112: Metagabbro, type A, coarse-grained variety. Same locality (1) as sample 114.
3. Sample 117: Metagabbro, type A, coarse-grained variety with well-developed coronas. Same locality (1) as sample 114.
4. Sample 118: Metagabbro, type A, fine-grained variety. Roadcut in the northwest side of Interstate 87, the last outcrop southbound from the exit to Route 9N in the metagabbro of the Hoisington Mountain intrusion.
5. Sample 36: Metagabbro, type A, coarse-grained variety. Roadcut at the southern end of Feeder Pond on the road from Witherbee to Underwood.
6. Sample 125: Metagabbro, type A. Roadcut on the western side of Interstate 87, first outcrop southbound from the rest area, about 3 km southeast from New Russia.
7. Sample 18: Metagabbro, type A. Roadcut on the eastern side of the road from Mineville to Elizabethtown, about 1 km north after crossing Lincoln Pond.
8. Sample 127: Metagabbro, type A. Roadcut on the western side of Interstate 87, about 3.7 km south from the rest area.
9. Sample 203: Metagabbro, type B. Southeast side of Interstate 87, the last outcrop southbound from the exit to Route 9N in the metagabbro of the Hoisington Mountain intrusion.
10. Sample 204: Metagabbro, type B. Same locality (9) as sample 203.
11. Sample 26: Metagabbro, type B. Northern side of the road from Witherbee to Underwood, Newport Pond.
12. Sample 41: Anorthositic metagabbro. Southern side of the road from Witherbee to Underwood, at Feeder Pond, about 0.5 km west from locality 5.
13. Sample 69: Woolen Mill granulite. Route 9N from Elizabethtown to Keene Valley, eastern end of Elizabethtown.
14. Sample 101: Anorthosite. Northeast side of Interstate 87, first outcrop southbound from the exit to Route 9N, about 7 km east of Elizabethtown.
15. Sample 9: Hybrid granitic gneiss. Roadcut on the southwest side of the road from Mineville to Elizabethtown, about 0.5 km northwest from Russet Pond.
16. Sample 198: Metagabbro relatively rich in SiO_2 due to assimilation of the country rock. Same locality (8) as sample 127.
17. Sample 196: Hybrid granitic gneiss. Roadcut on the southeast side of Interstate 87, first outcrop in the granitic gneiss south from Lincoln Pond.
18. Sample 194: Granitic gneiss with slightly increased mafic content. Same locality (17) as sample 196.
19. Sample 191: Granitic gneiss. Roadcut on the southeast side of Interstate 87, at Ash Craft Pond, about 4.5 km northeast from the exit to Keene Valley.
20. Sample 10: Granitic gneiss. Roadcut on the southwest side of the road from Mineville to Elizabethtown, about 1.3 km northwest from Russet Pond.

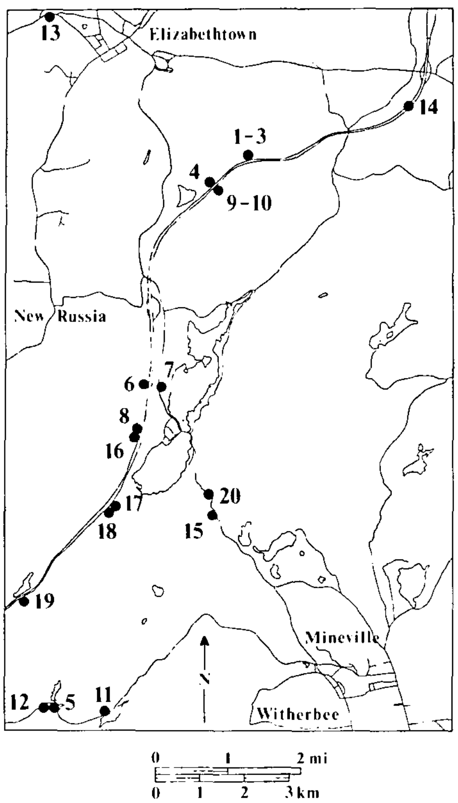

Appendix Figure 1. Localities of 20 samples from Elizabethtown quadrangle, analyzed for major elements.

REFERENCES CITED

de Waard, D., 1969, The anorthosite problem: The problem of the anorthosite-charnockite suite of rocks, *in* Isachsen, Y. W., ed., Origin of anorthosite and related rocks: New York State Museum and Science Service Memoir 18, p. 71–81.

de Waard, D., and Romey, W. D., 1969, Petrogenetic relationships in the anorthosite-charnockite series of Snowy Mountain Dome, south-central Adirondacks, *in* Isachsen, Y. W., ed., Origin of anorthosite and related rocks: New York State Museum and Science Service Memoir 18, p. 307–315.

Flanagan, F. J., 1973, 1972 values for international geochemical reference samples: Geochimica et Cosmochimica Acta, v. 37, p. 1189–1200.

Kemp, J. F., and Ruedemann, R., 1910, Geology of the Elizabethtown and Port Henry quadrangles: New York State Museum Bulletin, v. 138, 173 p.

Simmons, G., and Diment, W. H., compilers, 1973, Simple Bouguer gravity anomaly map of northern New York: New York State Museum and Science Service Map and Chart Series No. 17 A.

Walton, M. S., 1948–1960, Precambrian geology of the Elizabethtown and Paradox Lake quadrangles and the New York State portions of the Port Henry and Ticonderoga quadrangles: New York State Museum and Science Service.

Whitney, P. R., 1972, A layered intrusion near Jay Mountain, New York: Geological Society of America Abstracts with Programs, v. 4, p. 51.

Whitney, P. R., and McLelland, J. M., 1973, Origin of coronas in metagabbros of the Adirondack Mts., N.Y.: Contributions to Mineralogy and Petrology, v. 39, p. 81–98.

MANUSCRIPT RECEIVED BY THE SOCIETY AUGUST 6, 1979
MANUSCRIPT ACCEPTED AUGUST 15, 1979